SPATIO-TEMPORAL MEASUREMENTS OF CAPILLARY-GRAVITY WAVES

Paul A. Hwang¹, David W. Wang¹, Guillemette Caulliez², and Vladimir K.Makin³

¹Oceanography Division, Naval Research Laboratory, Stennis Space Center, MS, USA

²Air-Sea Interaction Laboratory, IRPHE-IOA, Marseille, France

³Royal Netherlands Meteorological Institute (KNMI), De Bilt, The Netherlands

<u>Summary</u> Small scale surface waves in the capillary-gravity region can be easily advected by surface currents from all sources. Temporal measurements using fixed-point wave probes, therefore, cannot resolve reliably the spatial or wavenumber structure of short waves unless the surface currents are also monitored, which is an even more difficult task than surface wave measurement. A two-dimensional scanning slope sensor system is developed to perform 4D measurements $[\nabla h(x,y,t)]$ of small scale surface waves. The data yield 3D spectrum $[B(k_x,k_y,w)]$ covering the capillary-gravity wave scales. The directional properties of small scale waves can be quantified by such data to a great detail. These data can be used to investigate the balance of source functions in the wave action conservation equation following the approach suggested by Phillips (1984, 1985).

A series of laboratory experiment is carried out to study the spectral properties of wind-generated waves in the capillary-gravity length scale. Two instruments are used for the wave measurements. The first is a two-dimensional laser scanning slope sensing system (SSS) similar to the one described by Hwang et al. (1993, 1996). The device scans a laser beam upward from underwater to cover a surface area of about $0.1 \text{ m} \times 0.1 \text{ m}$. The spatial resolution is 2 mm in both upwind and crosswind directions, and the temporal resolution is 50 frames per second. The second instrument is a linear array of 40 capacitance wave gauges (WGA) spaced 0.0508 m (2") apart, placed in the middle of the tank and with the gauges aligned in the downwind direction. The vertical resolution of the wave gauges is $2.3 \times 10^{-4} \text{ m}$. The wave gauges are simultaneously sampled with 40 analog-to-digital circuits at a rate of 50 Hz for each gauge.

An example of the slope topography obtained from the laser scanning system is shown in Fig. 1a for the upwind slopes. The spatio-temporal measurements can be analyzed to yield 3D saturation spectrum (Phillips 1985) of the surface waves $B(k_x,k_y,\mathbf{w})$, from which, 1D and 2D spectra can be calculated. Fig. 1b shows the 2D wavenumber spectrum $B(k_x,k_y)$ produced from integrating the 3D spectrum over frequency. The forward and backward propagating wave components can be clearly detected from $B(k_x,k_y)$. This is a significant improvement over the 2D wavenumber spectrum derived from individual images (denoted as $B'(k_x,k_y)$ here), in which the forward/backward and left/right information are not distinguishable due to the inherent axi-symmetric property of the Fourier transformation (Fig. 1c). The forward and backward propagating components appear in pairs within the resolution range of the instrument (k<1600 rad/m), with the upwind propagating waves having generally shorter wavelengths. The apparent upwind propagating components were originally thought to be the reflection of short waves in oscillating currents as described by Shyu and Phillips (1990). Unfortunately, later analysis indicates that they are a result of frequency aliasing because the sample rate (50 frames per second) is too slow and wave components with wavenumber greater than 500 rad/m may be misrepresented in the 3D spectrum. More quantitative analysis of the wave properties can be obtained from frequency slices of the 3D spectrum, an example is shown in Fig. 1d.

Phillips (1984) describes an approach to establish the dissipation function in the equilibrium region of gravity waves from the functional dependence of B on u_*/c , where u_* is the wind friction velocity and c is the wave phase speed. In particular, if B can be expressed as a power-law function of u_*/c , $B = A_0(u_*/c)^{a_0}$, and the dissipation function can be expressed as a power-law function of B, $D = A_d B^{a_d}$, then the coefficient and exponent of the dissipation function can be obtained from A_0 and a_0 , assuming local balance between the wind input and dissipation functions in the equilibrium region, and employing an empirically established wind input function. For shorter waves that are influenced by both gravity and surface tension, the balance of source/sink terms is much more complicated. For example, other generation and dissipation mechanisms, such as three-wave interaction, parasitic capillary wave generation, capillary wave reflection by orbital currents, micro scale breaking and viscous dissipation, may all be of the same order of importance in the energy and momentum balance of capillary-gravity waves. Phillips' approach, however, can still be applied to the analysis of the dynamic balance between the wind input and the D function, which is now treated as the sum of the remaining source/sink functions.

We examine the dependence of B on u_*/c in the capillary to short gravity wave region using both sets of SSS and WGA data. Indeed, the results appear to fit the power-law function nicely (Fig. 2a-b). The coefficient A_0 and exponent a_0 can be obtained from least square fitting of the measured data. The coefficient and exponent of the D function are calculated by A_d =0.04/ A_0 , and a_d =1+2/ a_0 . Fig. 2c shows the data-fitted a_0 as a function of the dimensionless wavenumber (normalized by k_m , the wavenumber of the wave component that gravitational force and surface tension force serve equally as the restoring force of the wave motion), and Fig. 2d shows the calculated a_d . Interestingly, the exponent of the D function varies only slightly in the capillary-gravity range. The average a_d is 1.54±0.37 from the SSS in the range of k/k_m >0.5, 1.38±0.16 from the WGA in the range of 1.2> k/k_m >0.4, and it gradually decreases to about 1 at k/k_m about

0.1. Compiling a dataset spliced from WGA measurements for k/k_m <0.9 and SSS measurements for k/k_m >1.1, and their average in the range $0.9 < k/k_m$ <1.1, a set of empirical equations is suggested for A_0 and a_0 for the convenience of computing the D function by A_d =0.04/ A_0 , and a_d =1+2/ a_0 (application range is approximately $5 > k/k_m$ >0.1):

$$A_0 = \begin{cases} 1.3 \times 10^{-2}, & k/k_m < 0.3 \\ 8.4 \times 10^{-4} (k/k_m)^{-2.3}, 0.3 \le k/k_m < 1.6 \\ 2.7 \times 10^{-4}, & k/k_m \ge 1.6 \end{cases}$$

$$a_0 = \begin{cases} 1, & k/k_m < 0.3 \\ \log[1.26(k/k_m)^{-3}], 0.3 \le k/k_m < 0.4 \\ 1.5, & k/k_m \ge 0.4 \end{cases}.$$

Phillips' (1984) approach is applied to short scale wave measurements collected in the ocean to study the source function balance of wind waves. The results suggest that the dissipation function is localized in the wavenumber space rather than the broadband distribution commonly assumed. The detail is described by Hwang and Wang (2004). References

- [1] Hwang, P. A., Trizna, D. B., Wu, J.: Dyna. Atmos. and Oceans 20:1-23, 1993.
- [2] Hwang, P. A., Atakturk, S., Sletten, M., Trizna, D. B.: J. Phys. Oceanogr 26:1266-1285, 1996.
- [3] Hwang, P. A., Wang, D. W.: Geophys. Res. Lett 31:L15301, doi:10.1029/2004GL020080, 2004
- [4] Phillips, O. M.: J. Phys. Oceanogr 24:1425-1433, 1984.
- [5] Phillips, O. M.: J. Fluid Mech 156:505-531, 1985.
- [6] Shyu, J.-H., Phillips, O. M.: J. Fluid Mech 217:115-141, 1990.

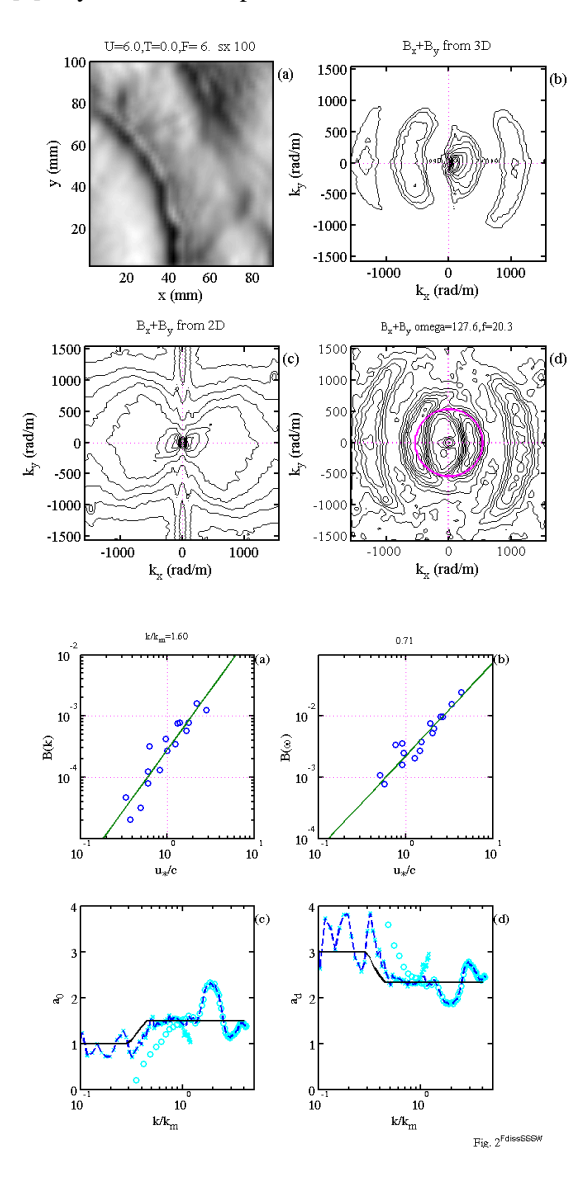


Fig. 1. Examples of the results from space-time measurements of capillary gravity waves using a laser scanning slope sensor system: (a) downwind slopes, (b) $B(k_x,k_y)$ integrated from 3D spectrum $B(k_x,k_y,\mathbf{w})$, (c) $B'(k_x,k_y)$ calculated from 2D images, and (d) the frequency slice of the 3D spectrum $B(k_x,k_y,\mathbf{w})$ at 20.3 Hz. In (d), the circle represents the linear dispersion relation for the given frequency. The spectra shown here are based on 30-s (1500 frames) average of the wave data collected at a fetch of 6 m, and the wind speed is 6 m/s. Contours plotted are 3 dB (about a factor of 2) apart. Positive k_x

is in the downwind direction.

Fig. 2.

Top row: Dependence of B on u_*/c , the solid curve is calculated from least square fitting. (a) From the scanning slope sensor data, (b) from the wave gauge array data. The results are obtained from 16 different combinations of wind speeds and fetches.

Bottom row: Empirically derived exponents of (c) $B(u_*/c)$, and (d) D(B). Circles are from SSS; crosses are from WGA. The spliced data are illustrated by the dashed curve and the suggested parameterization equations are shown by the solid curve.